A&A 454, 527–536 (2006)
DOI: 10.1051/0004-6361:20053468
© ESO 2006

Astronomy & Astrophysics

A search for photometric variability of hydrogen-deficient planetary-nebula nuclei⋆,⋆⋆

J. M. González Pérez[1,2], J.-E. Solheim[2,3], and R. Kamben[2]

[1] Instituto de Astrofísica de Canarias, 38200 La Laguna, Tenerife, Spain
e-mail: jgperez@iac.es
[2] Institut of Physics, University of Tromsø, 9037 Tromsø, Norway
[3] Institut of Theoretical Astrophysics, University of Oslo, PO box 1029 Blindern, 0315 Oslo, Norway

Received 18 May 2005 / Accepted 9 March 2006

ABSTRACT

Aims. We searched for photometric variability in a sample of hot, hydrogen-deficient planetary nebula nuclei (PNNi) with "PG 1159" or "O VI" spectral type, most of them embedded in a bipolar or elliptical planetary nebula envelope (PNe). These characteristics may indicate the presence of a hidden close companion and an evolution affected by episodes of interaction between them.
Methods. We obtained time-series photometry from a sample of 11 candidates using the Nordic Optical Telescope (NOT) with the Andalucía Faint Object Spectrograph and Camera (ALFOSC), modified with our own control software to be able to observe in a high-speed multi-windowing mode. The data were reduced on-line with the real time photometry (RTP) code, which allowed us to detect periodic variable stars with small amplitudes from CCD data in real time. We studied the properties of the observed modulation frequencies to investigate their nature.
Results. We report the first detection of low-amplitude pulsations in the PNNi VV 47, NGC 6852, and Jn 1. In addition, we investigated the photometric variability of NGC 246. Time-series analysis shows that the power spectra of VV 47, NGC 6852, and NGC 246 are variable on time scales of hours. Power spectra from consecutive nights of VV 47 and NGC 6852 show significant peaks in different frequency regions. The same type of variability is present in NGC 246 in 2 observing runs separated by 3 days. Changes are also found in the power spectra of VV 47 and NGC 246 during the same night. The VV 47 power spectra are peculiar since they present modulation frequencies in a wide range from 175 to 7600 μHz. This is different from the previously known pulsating PNNi where no frequencies are found above ∼3000 μHz. The high-frequency modulation observed in VV 47 may be due to g-modes triggered by the ϵ-mechanism, observed for the first time.

Key words. stars: oscillations – stars: individual: NGC 246 – stars: individual: VV 47 – stars: individual: NGC 6852 – stars: individual: Jn 1 – stars: AGB and post-AGB

1. Introduction

Pulsating planetary nebula nuclei (PNNi) constitute a class of non-radial pulsating degenerate stars. Ten PNNi are known to be non-radial pulsators (Grauer & Bond 1984; Bond & Meakes 1990; Ciardullo & Bond 1996; Vauclair et al. 2005). They show modulations with typical periods around 30 min and amplitudes ≲0.1 mag. The length and multiplicity of the periods indicate an origin in non-radial g-mode pulsations. The lowest modulation frequency observed for a PNN is 191 μHz (period 87.23 min), was observed in NGC 1501 (Bond et al. 1996), while the highest modulation frequency observed so far has been ∼2175 μHz (period 7.66 min) in RX J2117.1+3412 (Vauclair et al. 2002).

Ciardullo & Bond 1996 (hereafter CB96) have completed the most extensive search to date for pulsational variability among hydrogen-deficient PNNi with "O VI" and "PG 1159" spectral types. They identified 6 low-amplitude pulsators, including NGC 246, which is included in our sample. They found that the PNNi pulsational properties are similar to the pulsating GW Virginis (PG 1159-035) stars but tend to have longer pulsational periods (11.5 to 31 min) and that most of them have power spectra that vary on time scales of months or less. Furthermore, extensive observations, such as the detailed photometric study of NGC 1501 (Bond et al. 1996), show that a given pulsation changes its amplitude significantly and irregularly from night to night. Such instabilities could result from intrinsic variations in the star, but it could also be due to beats between modes that are closely spaced in frequency. Amplitude changes of peaks in the power spectra of PNNi have also been observed in completely resolved power spectra from long campaigns (see, e.g., Vauclair et al. 2002), so they must be real. This seems to be a property of the entire class. Most, if not all, of the pulsating PNNi show complex and variable behaviour. This is different from GW Vir white dwarf pulsators, whose power spectra are quite stable (Koupelis & Winget 1987; Winget et al. 1991; Kawaler et al. 1995) and which in general vary only on time scales of years.

These changes in the power spectra on time scales of months or less are not an exclusive characteristic of PNNi. Some pulsating DB white dwarfs (DBVs) also seem to have rapid variations. Handler et al. (2002) acquired 62 h of time-resolved

⋆ Based on observations obtained at the Nordic Optical Telescope, operated on the island of La Palma jointly by Denmark, Finland, Iceland, Norway, and Sweden, in the Spanish Observatorio del Roque de los Muchachos of the Instituto de Astrofísica de Canarias.

⋆⋆ The data presented here have been taken using ALFOSC, which is owned by the Instituto de Astrofísica de Andalucía (IAA) and operated at the Nordic Optical Telescope under agreement between IAA and the NBIfAFG of the Astronomical Observatory of Copenhagen.

Article published by EDP Sciences and available at http://www.edpsciences.org/aa or http://dx.doi.org/10.1051/0004-6361:20053468

Table 1. Targets: PNN spectral classification and nebula shape, where PN G indicates galactic-coordinate designations. The following coding is used for the nebula shape: bs (bipolar shape), es (elliptical shape), and us (unknown shape). The following coding is used for references of the spectra: N92, N93 (Napiwotzki 1992, 1993), NS95 (Napiwotzki & Schönberner 1995), W91 (Werner et al. 1991), and W92 (Werner 1992).

Object	PN G	m_v	Nebula	Spectrum	Ref. (spectrum)
PG 1520+525	85.4+52.2	16.6	us	PG 1159	W91
NGC 7094	066.7-09.5	13.68	es	"hybrid"	N92
				O(H,C)	N93
NGC 246	118.8-74.7	11.96	es	PG 1159/lgE	W92
NGC 6765	62.5+9.6	17.8	bs	O(C)	NS95
NGC 650-1	130.9-10.5	15.9	bs	PG 1159/E	N93
NGC 6852	42.59-14.53	18.2	bs	O(C)	NS95
Jn 1	104.2-29.6	16.13	bs	PG 1159/A:	W92
				PG 1159/E	N93
PN A 43	036.0+17.6	14.75	es	"hybrid"	N92
				O(H,C)	N93
IsWe 1	149.7-03.3	16.56	us	PG 1159/A:	W92
				PG 1159/A	N93
VV 47	164.8+31.1	16.83	bs	PG 1159/E:	W92
A 21	205.1+14.2	15.99	us	PG 1159/A:	W92
				PG 1159/E	N93

CCD photometry of the pulsating DBV PG 1456+103 and concluded that its pulsational spectrum is variable on time-scales of approximately 1 week.

To explain the PNNi pulsations, Starrfield et al. (1984, 1985) proposed a mechanism involving cyclical ionization and recombination of C and/or O in the outer layers of hot, hydrogen-deficient white dwarfs. This mechanism implies the existence of a C–O pulsational instability strip where the non-radial g-modes are triggered by the κ and γ mechanisms induced by this cyclical ionization-recombination process. However, it is not clear why the excited modes in PNNi change on time scales of months or less. One proposed explanation relates these changes to episodes of enhanced mass loss from the PNNi, which may alter the mode amplitude, since the driving zone for pulsations becomes closer to the surface (Bradley & Dziembowski 1996). This mechanism could explain the irregular change in amplitudes on a time scale of weeks, but cannot explain shorter time scales for amplitude changes, i.e., days.

An additional driving mechanism for g-modes during the PN and pre-white dwarf evolutionary phases is the ϵ-mechanism (Kawaler et al. 1986), which triggers g-modes because of a remnant He-burning shell. As the burning necessarily occurs at the bottom of the He-rich outer layers, the periods of these unstable g-modes are in the range of 70–200 s, corresponding to low k orders for $l = 1$ modes. Saio (1996) and Gautschy (1997) also found g-modes triggered by the ϵ-mechanism in some of their models with typical periods between ∼110 and ∼150 s. He-burning in the outer layers of a star is predicted to happen during the post-AGB stage (Asymptotic Giant Branch) in the evolution of single stars, but may also be the consequence of accreting helium from a helium-rich atmosphere of a close companion, like in the double-degenerated helium CVs (He CVs) (Warner 1995). In several of these cases the accretion produces an explosive ignition of the helium, but some remnant He may burn in a more static way (Iben & Tutukov 1991). Short-period g-modes excited by the ϵ-mechanism have not yet been observed.

In this paper we present a CCD survey for photometric variability in a sample of 11 PNNi selected as hot, hydrogen-deficient PNNi with "O VI" or "PG 1159" spectral type and a non-spherical planetary nebula envelope. These characteristics may be the result of the presence of a close companion and previous evolutionary phases with episodes of interaction between them. The spectroscopic class of PG 1159 stars consists of very hot hydrogen-deficient stars just entering the white-dwarf cooling sequence. The bipolar morphology of the nebulae may give indications of the presence of a binary system. Napiwotzki et al. (1996) found that the frequency of bipolar PNe in their sample of PG 1159 central stars is higher (75%) than what is found in other PNe samples (≤25%). This implies that binarity is important for the production of a PG 1159 star. In Sect. 2 we describe the targets and briefly discuss the selecion criteria. In Sect. 3 we describe the observations and the reduction procedures. In Sect. 4 we present our results, including the identification of 3 new pulsators: Jn 1, NGC 6852, and VV 47, and the rapid photometric variability observed for these objects and for NGC 246. We discuss the results in Sect. 5.

2. Target selection

Two parameters were taken into account for the selection of the PNNi sample: the existence of a "PG 1159" or "O VI" spectral type embedded in a preferably bipolar or even elliptical nebula with relatively low surface emission. However, this second parameter is not obvious in 3 candidates because the PNe are too faint. Table 1 summarises the main properties of the PNNi selected.

2.1. Spectral types

The spectral type selected is hot hydrogen-deficient PNNi. The spectral type "PG 1159" for PNNi was proposed by Schönberner & Napiwotzki (1990). They showed that several PNNi are spectroscopically indistinguishable from the PG 1159–035 white dwarfs, showing broad He II and C IV absorption lines near 4686 Å. This spectral type does not show the strong O VI emission that is the main characteristic of other hot hydrogen-deficient PNNi assigned to the "O VI" spectral type (Smith & Aller 1969; Heap 1982; Kaler & Shaw 1990).

The "O VI" class is defined by the presence of emission at O VI 3811–3834 Å. Heap (1982) proposed a more detailed classification scheme for the "O VI" spectral type to denote spectra that combine absorption lines with Wolf-Rayet WC-like emission features. A presumably evolutionary sequence, as well as

spectroscopic, has been suggested by Méndez et al. (1986). This sequence proceeds from WC-type spectra with strong emission lines, through transition objects like A 30 and A 78, which show absorption lines, as well as strong emission lines, and then to "O-type" objects with predominantly absorption lines plus weak emission spectra. This evolutionary sequence is completed with the PG 1159 spectral type. However, CB96 showed that the pulsational behaviour of PNNi is not consistent with this evolutionary sequence. So far no correlation has been found between PNN pulsators and no-pulsators and their spectral type. Pulsators have been found among all types of O VI central stars, from the WC through the PG 1159 spectral types.

In another clasification, Werner (1992) subdivided these PNNi into three subgroups depending on the He II and C IV lines appearance: "lgE" (low gravity emission) denotes objects that have relatively sharp absorption components underlying their He II and C IV emission (objects called O(C) in the Heap 1982 classification), and "E" (emission) denotes objects with higher gravity and with a mix of absorption and emission near 4686 Å. Finally the subgroup "A" indicates objects with pure 4686 Å absorption. Napiwotzki & Schönberner (1991) and Napitwotzki (1992, 1993) have identified several PNNi that appear to be "hybrid" PG 1159 objects in the sense that they show Balmer absorption lines in addition to their PG 1159 features. These hybrids are denoted "O(H, C)" by Napiwotzki (1993). The spectral types given in Table 1 are based on the classification scheme proposed by Werner et al. (1991), Werner (1992), and Napitwotzki (1992, 1993). The following coding is used: N92, N93 (Napiwotzki 1992, 1993), NS95 (Napiwotzki & Schönberner 1995), W91 (Werner et al. 1991), and W92 (Werner 1992).

2.2. Nebula shapes

The sample was completed selecting hydrogen-deficient PNNi embedded in a non-spherical planetary nebulae envelope. In general most of the PNe have complex but highly axisymmetric shapes. Only a small fraction (around 20%) show spherical symmetry. The majority of the PNe are either elliptical (around 30%) or bipolar (around 50%), including around 20% PNe with butterfly shape morphology (see, e.g., Zuckerman & Gatley 1998). Binary interactions (see, e.g., Fabian & Hansen 1979; Bond & Livio 1990; Han et al. 1995) provide a plausible mechanism for producing bipolarity. Han et al. (1995) conclude that binary interactions affect the shape of around 40% of all PNe. These results agree with previous studies of the formation of PNe and type Ia supernovae via various binary channels (e.g. Iben & Tutukov 1984, 1984, 1993; Tutukov et al. 1992; Yungelson et al. 1993, 1994).

Table 1 shows the type of nebulae of the PNNi selected in our sample. The following coding is used for the nebula shape: bs (bipolar shape); es (elliptical shape); us (unknown shape). The POSS E images from the Digitized Sky Survey show bipolar morphology for the PNe NGC 650-1, NGC 6765, Jn 1, and VV 47. At first glance NGC 6852 looks elliptical, but there is still a strong density contrast present between equatorial and polar directions, indicating a bipolar nature (Napiwotzki et al. 1996). POSS E images show that the PNe NGC 7094, NGC 246, and A 43 can be classified as elliptical. Filamentary structures are present in the three elliptical PNe. The PNe PG1520+525, IsWe 1, and A 21 are too faint or else interact with the interstellar medium in a way that makes classification difficult.

2.3. Other observations

Many of the selected PNNi (8 of 11) were also included in the CB96 survey. New observations of already checked candidates were decided because they present characteristics that fit one or both of our selection criteria and because the telescopes used in the CB96 survey were smaller (0.9 m and 1.5 m) than the Nordic Optical Telescope (2.56 m), which should give us a better chance to detect smaller amplitude pulsations.

The selected PNNi already observed by CB96 are: NGC 246, NGC 650-1, NGC 7094, A 21, A 43, IsWe 1, Jn 1, and VV 47. Among these, the authors only found evidence for coherent pulsations for NGC 246. Their data showed it to be an extremely low amplitude pulsator (around 2 mmag) with periods of 1440 s and 1860 s. More recently, Vauclair et al. (2005) have shown that A 43 is a pulsator and exhibits at least two periods of 2600 s and 3035 s. The other PNNi selected for monitoring in our survey were PG 1520+525, NGC 6765, and NGC 6852.

3. Observations and reductions

The observations were done at the 2.56 m Nordic Optical Telescope (NOT) with the Andalucía Faint Object Spectrograph and Camera (ALFOSC), equipped with a Loral, Lesser thinned, 2048×2048 CCD chip, and modified with our own control software to be able to observe in high-speed multi-windowing mode (Østensen & Solheim 2000). The sky area available for locating a reference star is limited to the sky area on the chip: 3.7×3.7 arcmin^2.

Table 2 contains the information related to the time-series observations. We observed the PNNi in windowed mode using two or more reference stars for constructing the relative light curve. Almost all the observations were made with a standard Bessell *B*-band filter (NOT #74, Bessell 1990). This filter minimized the contribution from the nebular emissions since many of the objects selected in our sample are embedded in low-surface-brightness nebulae. The sampling time (integration time plus readout time) varied from 30 to 180 s depending on the magnitude of the object. A typical run included one window for the target star, 2 or 3 for reference stars and 1 or 2 sky windows to compute sky levels.

The data were reduced on-line with the Real Time Photometry (RTP) code (Østensen 2000). This program allows us to detect periodic variable stars with small amplitudes from CCD data in real time. RTP plots the differential photometry light curves propagating in real time as the windowed frames are acquired from the CCD camera. At any point a Fourier Transform (FT) can be computed from the data acquired so far.

The CCD multi-windowed photometry method also gives us the opportunity to reprocess the data, applying different aperture sizes and correction schemes. The optimal combination of parameters as the size of the aperture, type of sky subtraction and ring width if annular sky subtraction is chosen, is selected as the one giving the lowest noise in the FT. The apertures tested ranged between 10 and 40 pixels in radius, which correspond to 1.9 and 7.6 arcsecs on the sky. The best results were obtained for relative small apertures (~10 to 15 pixels) using relatively large annular sky fields (~10 pixels). The data reduction procedure is completed with extinction corrections. After completing this procedure, and because the comparison stars were usually redder than the hot PNNi, we have a few long light curves which display long term trends. This may be the result of transparency variations, which affect the PNNi and the reference stars differently. Therefore, we do not consider as real those modulations

Table 2. Time-series photometry, with N_i denoting the number of independent samples, that is, the number of points in the light curve.

Object	Date	Start (UT)	Length (s)	Sampling (s)	N_i	Resolution (μHz)
PG 1520+525	2000 Jul. 20	20:39:59	6150	30	205	163
NGC 7094	2000 Jul. 20	23:55:25	5220	30	174	192
NGC 246	2000 Jul. 21	02:55:52	7448	33	255	134
	2000 Jul. 24	02:39:12	11 868	12	489	84
NGC 6765	2000 Jul. 21	21:24:55	6486	94,5	65	157
NGC 650-1	2000 Jul. 22	02:28:54	10 800	120	90	93
NGC 6852	2000 Jul. 22	23:50:42	10 800	180	60	93
	2000 Jul. 23	21:13:28	11 880	180	66	84
Jn 1	2000 Jul. 23	03:09:53	5695	85	67	176
A 43	2000 Jul. 24	01:13:52	4140	90	46	241
IsWe 1	2001 Jan. 15	20:30:59	13 547	50	270	74
VV 47	2001 Jan. 16	00:36:53	20 820	60	347	48
	2001 Jan. 16	21:04:03	22 560	60	376	44
	2001 Jan. 17	05:04:47	6360	60	106	157
	2001 Jan. 17	20:17:01	30 280	40	757	33
A 21	2001 Jan. 17	02:37:23	8000	40	200	125

with periods half of the run length or 1/3 of it, since they are most likely due to these changes.

In many of our observations, a run length of ∼1 h was enough to decrease the noise in the FT to less than 1 mma (where mma, the millimodulation amplitude, is the fractional amplitude in the FT in units of 10^{-3}). We could then decide if we wanted to observe the PNN longer or move to a new one. In cases where we suspected possible real modulations with quite low amplitude, we observed longer to improve the signal-to-noise ratio and thereby the chance to detect if peaks in the FT were real or not. Observations were repeated for objects suspected of having low-amplitude pulsations. This allowed us to confirm that the candidate had real periodic modulations and/or to study the daily changes in the power spectra.

The method used to estimate if a peak in the FT is real follows the procedure described by Kepler (1993). Following this method, a false alarm probability (FALSE) of 1/100 denotes that a peak will be considered real only if it has less than 1 possibility in 100 to be due to noise. The power needed to satisfy the criteria is given by the following equation:

$$P_{\rm obs} = \ln \frac{N_{\rm i}}{\rm FALSE} \langle P \rangle, \quad (1)$$

where N_i is the number of independent samples (points in the light curve), and $\langle P \rangle$ is the average power for the region of frequencies studied.

We selected a criterium using FALSE = 1/20. With this criterium, if a peak is over the estimated limit of confidence, it has less than 1 possibility in 20 to be due to noise. This criterium is chosen due to the following reasons: the periods that have been observed for PNNi have quite low amplitude (a few mma) and show temporal variability in the amplitude on different time scales. If this variability happens on shorter time scales than the length of the run, the amplitude in the FT for a certain peak, which is averaged over the whole run, may become less than significant. In other types of objects with stable power spectra this criterium may not be good enough, but this is not the case for the PNNi.

Considering $N_i = 200$, which is close to the number of independent samples obtained in many of our runs, $P_{\rm obs} = 8.3\langle P \rangle$. If the FT presents amplitudes, the peak must be 2.88 times over the average noise to be considered as real. Additional peaks with FALSE < 1/20 may be included only if: i) the frequency is equal to, or close enough to, the frequency of a significant peak observed in other runs, or ii) the ratio between pulsation frequencies with amplitudes at least 2 times over the noise (4 times in power) is close to 0.87. Ratios between pulsation frequencies close to this number have been observed in other PNNi and is predicted by the models related to non-radial g-modes. This ratio is described in Sect. 4.2.4.

4. Results

4.1. The non-pulsators

We did not find evidence of coherent pulsations in 7 of the 11 PNNi. No significant peaks were detected above the FAP with FALSE = 1/20, which is used as a criterium for all our observations. Table 3 presents the results obtained for these objects. The values for amplitudes are expressed in mma. The third column shows the amplitude of the highest peak in the FT. The fourth column presents the average amplitude in the FT. The fifth column displays the amplitude necessary for a FAP with FALSE = 1/20. Poor signal-to-noise ratios were obtained for fainter objects and those where the nebulae emissions were stronger. In these cases the use of smaller apertures in RTP helped to increase this ratio since it minimizes the sky contribution. Column 5 gives the FAP that indicates the quality of the data.

An example of the FT obtained for a non-pulsator (PG 1520+525) is presented in Fig. 1. Many of the runs for the non-pulsators were $\lesssim$2 h long, in order to search for periods near 30 min as expected from previous observations of PNNi. However, from such short runs, we cannot detect possible variability happening on time scales >∼1 h.

Some of our observations confirm the null results obtained previously by CB96 but after improving the threshold. For example, the highest peak observed in our FT for IsWe 1 has an amplitude of ∼1 mma, and the average amplitude is 0.41 mma. The amplitude of the highest peak found in the "noise" in CB96's best run was 3.4 mmag. On the other hand, Vauclair et al. (2005) demonstrate that A 43 is a pulsator that exhibits at least two frequencies of 329 and 384 μHz with amplitudes of 2.1 and 2.4 mma.

Based on these observations, we cannot claim that these objects are non-pulsators. We can only conclude that they do not show coherent pulsations satisfying our detection criteria when

Table 3. Results for non-pulsators.

Object	Length run (s)	Max. amplitude (mma)	Average amplitude (mma)	FAP (mma)
PG 1520+525	6150	≲1	0.50	1.44
NGC 7094	5220	≲0.7	0.32	0.91
NGC 6765	6486	1.5	0.66	1.77
NGC 650-1	10 800	≲3	1.32	3.61
A 43	4140	≲3	2.30	6
IsWe 1	13 547	≲1	0.41	1.20
A 21	8000	0.8	0.36	1.04

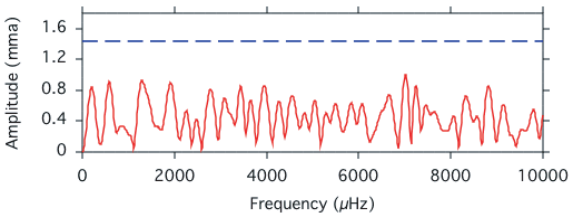

Fig. 1. PG 1520+525 FT from NOT data. The dashed line is the FAP limit.

they were observed. The PNNi may have shown variability during the observations, but with amplitudes below this threshold. Previous observations of some pulsating PNNi have revealed that in some cases the light curves occasionally exhibit intervals where variations nearly disappear. Observations during these intervals may not show any detectable coherent pulsations.

4.2. The pulsators

In general, the peaks found in the FTs that are candidates for possibly real modulation frequencies in our PNN sample have low amplitudes and were variable on time scales of days or hours. These facts make it difficult to conclude if those peaks in the FT were due to real pulsations or not. The noise in the FT decreases by increasing the length of the observation. For a stable pulsation, it is easy to identify a real peak by observing until the FT signal-to-noise ratio satisfies our FAP criterium. This may not be possible if the periodic modulations change in amplitude on time scales of hours; a short run may produce a peak that may satisfy our criterium, but as the run continues, this real modulation frequency may reduce its amplitude. Use of FT detects only pulsations that are stable in time. Therefore, the FT over the whole run may show a small peak above the noise, which does not satisfy our criterium for a real peak. The on-line analysis done with RTP helps somewhat, since we can constantly monitor the FT of the data acquired so far. Therefore, we can follow how peaks that appear during the first part of the observation evolve with time.

4.2.1. Jn 1

CB96 included Jn 1 in their survey. Their data show possible peaks at 540.5 and 538.5 μHz, but the level of confidence was not very high so they did not claim variability. Our analysis suggests variability of this PNN with bipolar envelope. However, the results are at the limit of our confidence criterium, and the length of the run was only 1.58 h. However, this length was enough to reach an average noise amplitude of 0.36 mma. In this case the FAP amplitude is 0.97 mma. We detected a peak at 2200 μHz just at this level (1.01 mma). Our data do not show power near the suspected peaks at 540.5 and 538.5 μHz reported by CB96, but the 2200 μHz peak may be a 3rd harmonic of one of these. This strengthens the indication that the peak at 2200 μHz might be real. Harmonics are observed in systems with discs, and the fundamental period is the superhump or orbital period (Solheim et al. 1998). In this case we may have an orbital period of ~30 min. More observations are needed to confirm this.

4.2.2. NGC 246

The bright (V = 11.77) central star of NGC 246 is listed as a photometric standard star by Landolt (1983) and as a non-variable by Grauer et al. (1987). CB96 showed it to be a low amplitude pulsator with periods of 24–31 min and amplitude of ~2 mmag. They observed this object on 3 different nights. Significant peaks were detected at 683 and 648 μHz in the power spectra of the first two runs, which were consecutive nights. A third run was obtained 9 months later and showed a different peak at a lower frequency (540 μHz). It should be noted that the central star of NGC 246 has a K-dwarf companion star located 3.8 arcsec away (Bond & Ciardullo 1999). Both stars were included in the aperture photometry measurements.

We included this PNN in our sample in order to monitor possible changes in the power spectra. We observed it a total of 5.36 h, divided in two runs: the first run was held on 2000 July 21 and only lasted for 2.07 h. The second run was done 3 nights later and lasted for 3.30 h. The sampling time was reduced from 33 s in the first run to 12 s in the second. In order to reach a shorter sampling time, we decreased the exposure time some. Therefore, the light curve for the second run is slightly noisier.

In the following, the FTs are displayed in power (μmp) instead of amplitude. We used this unit for the objects observed at least two nights and also that showed possible pulsations. The power unit makes it easier to compare different FTs when looking for changes on time scales of days or less. Therefore, the FAP is also in μmp. The light curves are presented in Fig. 2.

The average power obtained is low in these runs: ~0.1 μmp in both power spectra. The FAP is 0.85 μmp for the first run and 0.92 μmp for the second. The power spectra show two regions of enhanced power with low amplitude that varies from the first to the second run (see Fig. 3). The power of these 2 peaks satisfies our confidence criterium. The first run shows power only in one region ~550 μHz (power: 3.7 μmp), while the second run shows a peak with less power (1.8 μmp) in the same region and, in addition, a new main peak at ~685 μHz (5.6 μmp), which is absent in the first run. Power at the level of the confidence criterium is also found at ~230 μHz (0.9 μmp). Analysis of the second run indicates that all the pulsation power is concentrated in the last part of the run (see Fig. 4).

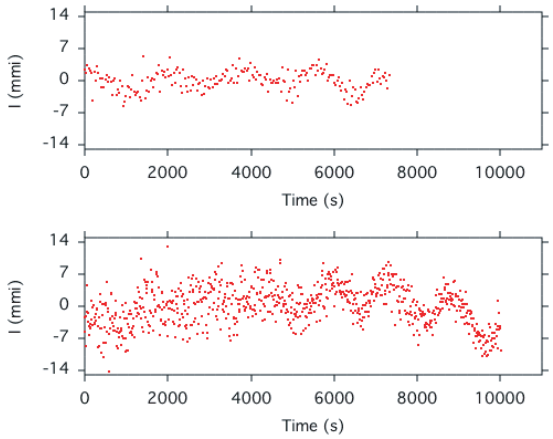

Fig. 2. NGC 246 light curves from NOT data: the upper panel shows the light curve of the July 21st (2000) run and the lower panel the light curve of the July 24th (2000) run.

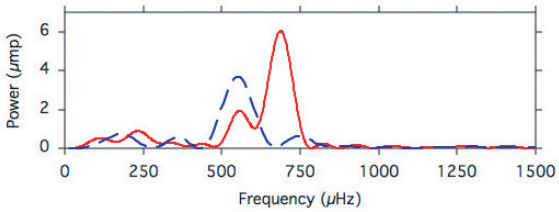

Fig. 3. Comparison of NGC 246 temporal spectra from NOT data. The dashed line is the temporal spectrum of the July 21st run and the continuous line the temporal spectra of the July 24th run.

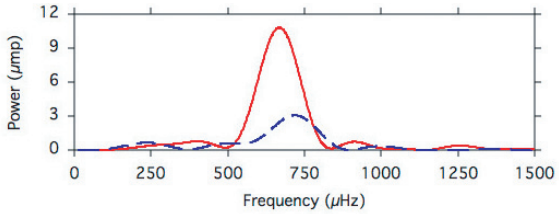

Fig. 4. Comparison of NGC 246 FTs from July 24st NOT data. The dashed line is the FT of the first half part of July 24st run and the continuous line the FT of the second half.

Daily changes in the power spectra have been observed before in other PNNi but as amplitude variations. This time we observed the appearance of a modulation frequency completely absent in the previous data set taken 3 days earlier. CB96 also found significant peaks in the same frequency region changing from run to run. However, the variations in the power spectra reported were from runs spaced by many months, in contrast to our 3-days separation.

4.2.3. NGC 6852

We observed this faint PNN with bipolar PNe and PG 1159 spectral type 6.3 h in two runs over consecutive nights: the first lasted for 3 h and the second was obtained ~18 h later and lasted for 3.3 h. We found no evidence of pulsational variability in the first run.

The power spectrum of the second run shows two regions with enhanced power (see Fig. 5). A peak with power 7.6 μmp is seen around 912 μHz (period: 1088 s); the FAP around this frequency is 6.5 μmp. Therefore, this peak satisfies the confidence criterium. An additional peak with power 5.9 μmp is present at

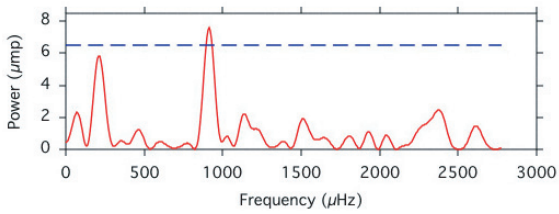

Fig. 5. NGC 6852 FT from July 23rd NOT data.

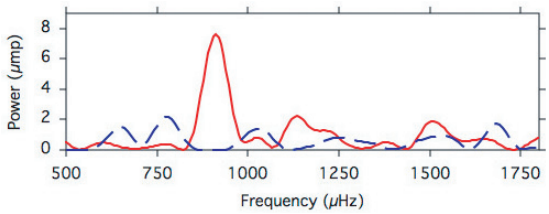

Fig. 6. Comparison of NGC 6852 FTs from NOT data. The dashed line is the FT of the July 22nd run and the continuous line the FT of the July 23rd run, 18 h after the first run.

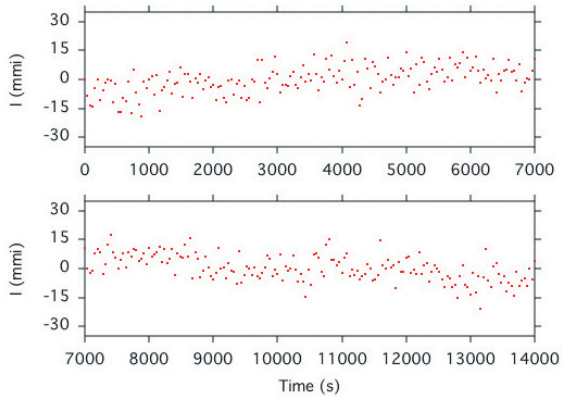

Fig. 7. VV 47 light curve from the last run.

210 μHz. This corresponds to a period of 5128 s. The length of this run was 11 880 s, which is close to two times this suspected modulation period. Longer light curves must be obtained to check whether this modulation is real or not.

Figure 6 presents a comparison of the power spectra from both runs near the peak at 912 μHz. It shows that this peak is not present in the power spectrum of the first run. As in the NGC 246 case, we find a modulation frequency absent in a previous observation. In this case the time between the two runs is even shorter: 18 h.

4.2.4. VV 47

Liebert et al. (1988) reported possible short-period variability for this object on the basis of aperture photoelectric photometry. CB96 included it in their survey. They observed this PNN for 12.7 h over 4 nights but could not confirm the suggested variability. We included it in our sample because of our higher sensitivity, and it satisfies the selection criteria. We got 22.2 h of data divided into 4 runs on three consecutive nights. Figure 7 shows the VV 47 light curve obtained in the last run.

The length of the first run was 5.8 h. The average power is 0.15 μmp and the FAP becomes 1.35 μmp. The power spectrum obtained for the low-frequency region is presented in Fig. 8 (first panel from the top), and for the high-frequency region in

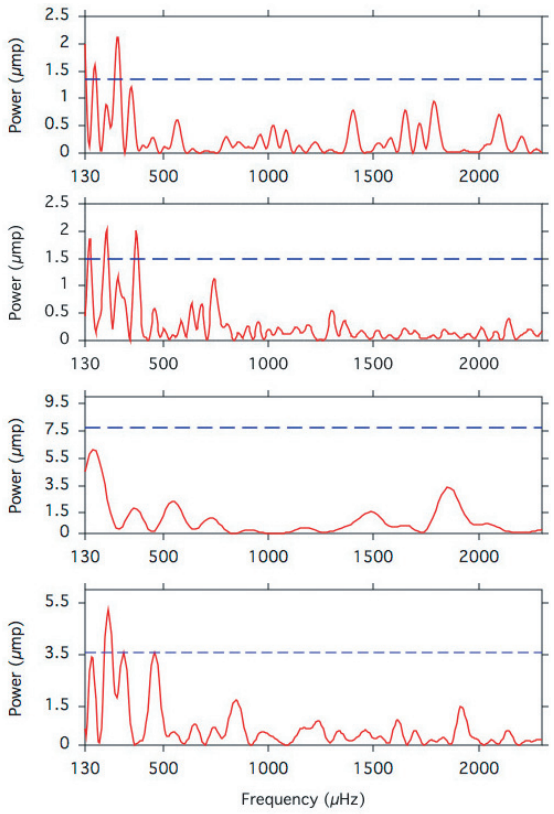

Fig. 8. VV 47 low-frequency region power spectra from different runs. Notice that the vertical axis scales are different. The dashed lines are the FAP limit.

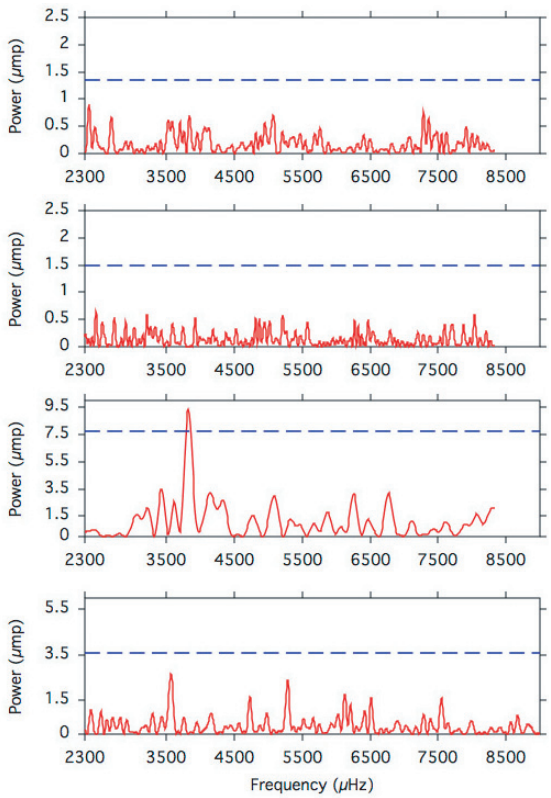

Fig. 9. VV 47 high-frequency region power spectra from different runs. Notice that the vertical axis scales are different. The dashed lines are the FAP limit.

Fig. 9 (first panel from the top). Two peaks are found above the FAP limit: 176 μHz (1.6 μmp) and 284 μHz (2.1 μmp). The peak at 284 μHz is a good candidate for a real modulation frequency since the associated power clearly satisfies the confidence criterium. A small peak appears in the region of the first harmonic: 565 μHz (0.6 μmp). Taking the resolution of the run into account, power is also found in the region related to 176 μHz first harmonic: 348 μHz (1.2 μmp). Another small peak is found at ~232 μHz (0.9 μmp). Its level of significance is not high, but we mention it since power is found again near this frequency in the other long runs.

The second run on VV 47 was obtained ~14 h later. The length of the run was slightly longer: 6.27 h. The average power for this run is 0.17 μmp and the FAP becomes 1.49 μmp. The power spectrum obtained for the low frequencies region is presented in Fig. 8 (second panel), and for the high frequencies region in Fig. 9 (second panel). Three peaks are found to satisfy the FAP criterium: 150 μHz (1.9 μmp), 232 μHz (2 μmp), and 373 μHz (2 μmp). We do not want to claim the peak at 150 μHz is real because its amplitude depends on the reference star selected for the differential photometry. The peak at 232 μHz is a strong candidate for a real modulation frequency since it satisfies the confidence criterium in this run and it is present in others.

The third run was obtained the same night 1.5 h after the second one. This is a short run of 1.77 h. Therefore, the average power is higher than in the previous cases: 1.03 μmp and FAP 7.78 μmp. A peak satisfying the confidence criterium is present at 3826 μHz (9.4 μmp). The power spectrum obtained for the low-frequency region is presented in Fig. 8 (third panel) and for the high-frequency region in Fig. 9 (third panel).

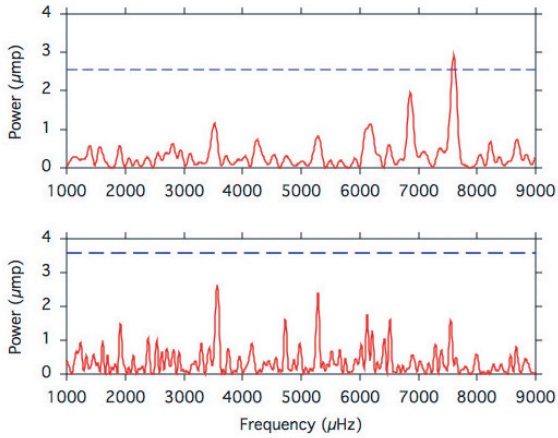

Fig. 10. VV 47 FTs comparison from the first section of the last run (*upper panel*) and the complete last run (*lower panel*). The dashed lines are the FAP limit. The peak at 7604 μHz in the upper panel is near the first harmonic of the peak observed in run 3. Notice that this peak is over the FAP, if we consider only the first section, but decreases in amplitude and is below the FAP, if we consider the complete run.

The last run on VV 47 was obtained during the next night, ~13 h after the previous one. In this case a high peak, which appeared during the first part of the run, started to decrease in amplitude after ~2.5 h observing. Therefore, we calculated the FT for the first section (2.32 h) and for the whole run separately (see Fig. 10). The average power for the first section is 0.33 μmp, which gives an FAP of 2.5 μmp. A peak present at 7597 μHz satisfies the criterium with power 2.9 μmp. An important characteristic of this peak is that it is near the region of the first harmonic

Table 4. Interesting peaks in VV 47 power spectra. The following coding is used for the last column: the number 1 indicates that a peak has a related harmonic or is itself harmonic of a significant peak present in the same run. The number 2 indicates that a peak has a related harmonic or is the harmonic of a significant peak present in another run. The number 3 indicates that a peak satisfies the ratio $\mathcal{R}$ with another peak. Bold indicates peaks with best chances to be real.

Freq. (μHz)	P (s)	Run	FAP (μmp)	Power (μmp)	Over FAP?	More
~176	5682	1	1.48	1.6	yes	1
~**232**	4310	1	1.48	0.9	no	2
		2	1.68	2.0	yes	2
		5	4.01	5.2	yes	1
~**284**	3521	1	1.48	2.1	yes	2
		2	1.68	1.2	no	
~348	2874	1	1.48	1.2	no	1
~**373**	2681	2	1.68	2.0	yes	1
~**460**	2174	5	4.01	3.6	no	2
~742	1348	2	1.68	1.1	no	1
~847	1181	5	4.01	1.7	no	2
~3570	280.1	5	4.01	2.7	no	3
~**3826**	261.4	3	8.90	9.4	yes	
~4159	240.4	3	8.90	3.2	no	
		5	4.01	0.9	no	3
~4731	211.4	5	4.01	1.6	no	3
~5286	189.2	5	4.01	2.4	no	3
~6127	163.2	5	4.01	1.8	no	3
~6516	153.5	5	4.01	1.6	no	3
~7550	132.5	5	4.01	1.6	no	3
~7597	131.6	4	3.01	2.9	no	2

of the peak observed in the previous run. However, no power is found near its possibly fundamental period.

The length of the complete run is ~4 h. The complete last-run power spectrum obtained for the low-frequency region is presented in Fig. 8 (bottom panel), and for the high-frequency region in Fig. 9 (bottom panel). The average power is 0.42 μmp, which gives an FAP of 3.57 μmp. The average noise is higher than for the first section of the run. This may be due to deteriorating observing conditions. Two peaks satisfy the confidence criterium: 240 μHz (5.2 μmp) and 460 μHz (3.6 μmp). Power in the region ~240 μHz is found in the two other long runs. Power at the confidence level is present in the area close to the first harmonic: 460 μHz (3.6 μmp).

In general, no peaks above the confidence level are found at frequencies higher than ~500 μHz in this run. The power of the peak at 7597 μHz, present in the FT of the first section of the run, is significantly reduced in the complete set, but some power is still present above the local noise. However, some of the higher peaks present above 3000 μHz may be real since the period ratio between them fits $\mathcal{R}$ = 0.87. This property can be explained as follows: the period spacing observed in GW Vir itself is not precisely constant (Winget et al. 1991; Kawaler & Bradley 1994). These authors note that this could result from mode trapping, as a subsurface composition transition region can cause a density discontinuity that acts as a reflecting boundary between the surface and the deep stellar interior. Kawaler & Bradley (1994) identify this layer as the transition zone between the helium-rich surface layer and the carbon/oxygen core. The authors present the periods of trapped modes in their Eq. (4) and the trapping coefficients λ_i for PG 1159 stars in their Table 2. They conclude that if trapped modes are identified in a star, then the period ratios between the modes can be compared with these coefficient ratios. Many of these ratios are close to the value $\mathcal{R}$ = 0.87.

The higher peaks found in the FT of the VV 47 last run in the interval over 3000 μHz are 3570 μHz (2.7 μmp), 4731 μHz (1.6 μmp), 5286 μHz (2.4 μmp), 6127 μHz (1.8 μmp), 6516 μHz (1.6 μmp), and 7550 μHz (1.6 μmp). All these peaks are $\gtrsim$4 times the average noise in power. Taking the resolution of the run (69 μHz) into account, the ratios 5286/6127 and 6516/7550 fit $\mathcal{R}$. Additional power is found at 4159 μHz (0.9 μmp). The ratios 3570/4159, 4159/4731, and 4731/5286 are also close to $\mathcal{R}$.

Table 4 presents a summary of the significant peaks found in the different runs. The power and the FAP are expressed in μmp. The second column lists the associated periods. A "yes" in the sixth column indicates that the power of the peak of this modulation frequency satisfied the FAP. The last column shows other criteria used: the number 1 indicates that a peak has a related harmonic or is itself harmonic of a significant peak present in the same run. The number 2 indicates that a peak has a related harmonic or is the harmonic of a significant peak present in another run. The number 3 indicates that a peak satisfies the ratio $\mathcal{R}$ with another peak. Bold indicates peaks with best chances to be real.

Our analysis suggests that the VV 47 is a low-amplitude pulsator showing an extremely complicated power spectrum. In general the most significant peaks have highly variable amplitudes from run to run or are only found in one of them. Power is found covering a wide range of frequencies. Possibly real peaks may exist from 175 μHz to 7600 μHz. The peak found during the last run at 7597 μHz satisfies the confidence criterium only in the first part of the run but is far below the limit if we consider the whole run. This may indicate a short life time for these modulations, maybe only a few hours.

Evidence of ϵ-mechanism in VV 47?

Our analysis of VV 47 photometry indicates the presence in the high frequency range of some possibly real peaks candidates for low-k order g-modes driven by the ϵ-mechanism. The highest peak found during the third run at 3826 μHz may be a good candidate. In addition, we have mentioned the presence of peaks over at least four times the average power at frequencies above 3000 μHz, which do not satisfy the FAP confidence criterium but other criteria such as the ratio between them fitting $\mathcal{R}$. Such

a criterion indicates that these peaks may be candidates for g-modes and, due to their high frequencies, triggered by the ϵ-mechanism. However, these peaks are found in only one of our long runs. They may be present in others but with lower amplitudes and confused with noise. If those peaks are real, the ϵ-mechanism that is supposed to trigger them is quite unstable and generates g-modes that vary in amplitude on time scales of hours.

Interaction with a close companion?

We have found peaks that could be harmonics of significant peaks, both in the same FT or in FT of other runs. These harmonics are observed in systems with accretion discs. The harmonics in these systems modulate the light curve strongly. In an extreme case, such as in the power spectra of AM CVn, harmonics are present in the FT, but the fundamental modulation frequency is not generally observed (Solheim et al. 1998). This is explained by symmetries in the physical structure of the accretion discs. Harmonics are also observed related to normal modes in other pulsating PNNi. In this case they are pulse shape harmonics of non sinusoidal pulsations, and the fundamental modulation frequency is always present in the FT.

Comparing the different power spectra obtained for VV 47, we have found possible indications of interaction with a close companion. The best candidate is the peak at ~230 μHz, found in runs 1, 2 and 5. Significant power is found in the region of its first harmonic but only during the run 5. Other examples are indicated in the last column of the Table 4: the number 1 indicates that a peak has a related harmonic or is itself harmonic of a significant peak present in the same run, in which case we may be observing pulse shape harmonics. The number 2 indicates that a peak has a related harmonic or is the harmonic of a significant peak present in another run, in which case we may be observing symmetries developed due to interaction with a close companion.

5. Discussion

We have completed a survey looking for pulsational variability in a sample of 11 PNNi selected by the following criteria: "PG 1159" or "O VI" spectral type and a bipolar or elliptical planetary nebula envelope (PNe). These characteristics suggest the possible presence of a close companion. We reported the discovery of three new pulsators: Jn 1, VV 47, and NGC 6852. Our results increase the number of known pulsating PNNi to 13: A 43, RX J2117.1+3412, NGC 1501, NGC 2867, NGC 2371-2, NGC 6905, NGC 5189, Lo 4, K 1-16, NGC 246, NGC 6852, VV 47, and Jn 1. In general, all our pulsators show low-amplitude modulation frequencies and a complex photometric behaviour that both change on short time scales: NGC 246 presents significant changes between two runs 3 days apart, with the appearance of a ignificant peak at 685 μHz completely absent in the first run. The analysis of the second run of NGC 246 indicates that all the pulsation power is concentrated in the last part of the run. This behaviour is peculiar since the daily changes observed previously in other PNNi are variations in the amplitudes of certain peaks, but never the appearance of a new peak. Our runs are not long ($\leq$4 h), so one possible explanation could be the beating of close modes in an unresolved power spectrum. However, changes in amplitude have also been reported in completely resolved power spectra for others PNNi, such as RX J2117.1+3412 (Vauclair et al. 2002). This result indicates that the observed changes in NGC 246 may be real.

The evolutionary time scales in the PNN phase is very short, and processes like mass loss may alter the amplitude of the PNNi g-modes on time scales of weeks. However, this mechanism seems to be insufficient for explaining the observed variations in NGC 246, which occur on time scales of days or less. The same behaviour was observed in the PNN NGC 6852. We observed this PNN for two consecutive nights. The FT from the first run does not show any evidence of pulsations, but a second run obtained only 18 h later showed a significant peak at ~910 μHz. These rapid variations imply time scales that are difficult to explain by processes happening inside the star. Another option is to explain them by involving processes related to interactions with a close companion. These processes introduce changes on a dynamical time scale, like the creation of an accretion disc and onset of mass transfer that may modulate the light curves. The presence of a disc can be supported by typical signatures of CVs with accretion discs. Those are the presence of several harmonics of a main period, which is associated to the shape and dynamics of the accretion disc. The main periods may be the orbital period, the superhump period, or the period of rotation. We have searched for such features but have not found harmonics to the changing modulation frequencies for NGC 246 and NGC 6852. On the other hand, the only peak that satisfied the confidence criterium for Jn 1 (2200 μHz) may be a 3rd harmonic of one of the suspected peaks at 540.5 and 538.5 μHz reported by CB96.

VV 47 exhibits even more complicated and variable power spectra. We followed this object for 3 consecutive nights and obtained pulsations covering a wide range of frequencies: from 176 μHz to 7597 μHz. This is the first time that possible modulation frequencies for a PNN above ~2175 μHz have been found. The power spectrum is again quite variable from night to night but some modulation frequencies at lower frequencies are present in at least two long runs (232 μHz and 284 μHz). Power is also found near the first harmonic of 232 μHz and the second harmonic of 284 μHz. The high frequency region for this object is quite interesting. The first long run did not show evidence of pulsations in this range. However, in the third short run a significant peak appeared at 3826 μHz. Additional low-amplitude pulsation g-mode candidates appeared in the region above 3500 μHz in the last run. Therefore, this may be the first time that we have observed candidates for low-k order g-modes driven by the ϵ-mechanism. The complex power spectra of this PNN may indicate a combination of processes going on around the star plus normal oscillation modes of the star. However, they are unstable, changing quickly with time.

In general, the new pulsators discovered and the rapid changes in the power spectra obtained for them and for NGC 246 suggest the necessity of introducing additional tools for analysis, such as wavelets. The Fourier analysis seems inappropriate for analysis of these light curves, since it considers that all the modulation frequencies are static and have constant amplitudes. The rapid changes also indicate that the search for new PNN pulsators is complicated, since one must monitor a candidate repeatedly to be certain it pulsates. Confidence criteria based on the presence of significant power at the same frequency in all runs do seem not to be appropriate either. In addition, the search for peaks filling the confidence criterium must be done by carefully analysing not only the complete run but sections of it. An example is the peak at 7597 μHz obtained in the fourth run on VV 47, which is the first harmonic of the significant peak found in the third run. This peak satisfied the confidence criterium during the

first half of the run, but decreased in amplitude and did not satisfy the confidence criterium when considering the whole run. This change suggests that processes on timescales of ∼2 h happen in the star.

References

Bessell, M. S. 1990, PASP, 102, 1181
Bond, H. E., & Livio, M. 1990, ApJ, 355, 568
Bond, H. E., & Meakes, M. G. 1990, AJ, 100, 788
Bond, H. E., Kawaler, S. D., Ciardullo, R., et al. 1996, AJ, 112, 2699
Bond, H. E., & Ciardullo, R. 1999, PASP, 111, 217
Bradley, P. A., & Dziembowski, W. 1996, ApJ, 468, 350
Ciardullo, R., & Bond, H. E. 1996, AJ, 111, 2332 (CB96)
Fabian, A. C., & Hansen, C. J. 1979, MNRAS, 187, 283
Gautschy, A. 1997, A&A, 320, 811
Grauger, A. D., & Bond, H. E. 1984, ApJ, 277, 211
Grauer, A. D., Bond, H. E., Liebert, J., et al. 1987, ApJ, 323, 271
Han, Z., Podsiadlowski, P., & Eggleton, P. P. 1995, MNRAS, 272, 800
Handler, G., Metcalfe, T. S., & Wood, M. A. 2002, MNRAS, 335, 698
Heap, S. R. 1982, in Wolf-Rayet Stars: Observations, Physics, Evolution, ed. C. W. H. de Loore, & A. J. Willis (Reidel, Dordrecht), IAU Symp., 99, 423
Iben, I., Jr., & Tutukov, A. V. 1984a, ApJS, 54, 335
Iben, I., Jr., & Tutukov, A. V. 1984b, in Stellar Nucleosynthesis, ed. C. Chioso, & A. Renzino (Dordrecht: Reidel), 181
Iben, I., Jr., & Tutukov, A. V. 1991, ApJ, 370, 615
Iben, I., Jr., & Tutukov, A. V. 1993, ApJ, 418, 343
Iglesias, C. A., & Rogers, F. J. 1993, ApJ, 412, 752
Kaler, J. B., Shaw, R. A., & Kwitter, K. 1990, ApJ, 359, 392
Kawaler, S. D., & Bradley, P. A. 1994, ApJ, 427, 415
Kawaler, S. D., Winget, D. E., Hansen, C. J., & Iben, I., Jr. 1986, ApJ, 306, L41
Kawaler, S. D., O'Brien, M. S., Clemens, J. C., et al. 1995, ApJ, 450, 350
Kepler, S. O. 1993, Baltic Astron., 2, 515
Koupelis, T., & Winget, D. E. 1987, in The Second Conference on Faint Blue Stars, ed. A. G. D. Philip, D. S. Hayes, & J. W. Liebert (Schenectady: Davis), IAU Coll., 95, 623
Landolt, A. U. 1983, AJ, 88, 439
Liebert, J., Fleming, T. A., Green, R. F., & Grauer, A. D. 1988, PASP, 100, 187
Mendez, R. H., Miguel, C. H., Heber, U., & Kudritzki, R. P. 1986, in Hydrogen-Deficient Stars and Related Objects, ed. K. Hunger, et al. (Dordrecht: Reidel), 323
Minkowski, R. 1965, in Galactic Structure, ed. A. Blaauw, & M. Schmidt (Chicago: university of Chicago Press), 321
Napiwotzki, R. 1992, in The Atmospheres of Early-Type Stars, ed. U. Heber, & C. S. Jeffery (Berlin: Springer), 310
Napiwotzki, R. 1993, Acta Astron., 43, 343
Napiwotzki, R., & Schönberner, D. 1991, A&A, 249, L16
Napiwotzki, R., & Schönberner, D. 1995, A&A, 301, 545
Napiwotzki, R. Haas, S., Schönberner, D., et al. 1996, in Hydrogen-Deficient Stars, ed. C. S. Jeffery, & U. Heber, ASP Conf. Ser., 96, 213
Saio, H. 1996, in Hydrogen-Deficient Stars, ed. C. S. Jeffery, & U. Heber, ASP Conf. Ser., 96, 361
Schönberner, D., & Napiwotzki, R. 1990, A&A, 231, L33
Smith, L. F., & Aller, L. H. 1969, ApJ, 157, 1245
Solheim, J.-E., Provencal, J. L., Bradley, P. A., et al. 1998, A&A, 332, 939
Stanghellini, L., Cox, A. N., & Starrfield, S. G. 1991, ApJ, 383, 766
Starrfield, S., Cox, A. N., Kidman, R. B., & Pesnell, W. D. 1984, ApJ, 281, 800
Starrfield, S., Cox, A. N., Kidman, R. B., & Pesnell, W. D. 1985, ApJ, 293, L23
Tutukov, A. V., Yungelson, L. R., & Iben, I., Jr. 1992, ApJ, 334, 357
Vauclair, G., Moskalik, P., Pfeiffer, B., et al. 2002, A&A, 381, 122
Vauclair, G., Solheim, J.-E., & Østensen, R. 2005, A&A, in press
Warner, B. 1995, Ap&SS, 225, 249
Werner, K. 1992, in The Atmospheres of Early-Type Stars, ed. U. Heber, & C. S. Jeffery (Berlin: Springer), 273
Werner, K., Heber, U., & Hunger, K. 1991, A&A, 244, 437
Winget, D. E., Nather, E. R., Clemens, J. C., et al. 1991, ApJ, 378, 326
Yungelson, L. R., Tutukov, A. V., & Livio, M. 1993, ApJ, 418, 794
Yungelson, L. R., Livio, M., Tutukov, A. V., & Saffer, R. A. 1994, ApJ, 420, 336
Zuckerman, B., & Gatley, I. 1988, ApJ, 324, 501
Østensen, R. 2000, Time Resolved CCD Photometry, Ph.D. Thesis, University of Tromsø
Østensen, R., & Solheim, J.-E. 2000, Baltic Astron., 9, 411